Scanning Microscopy

Volume 6 | Number 2 Article 2

4-6-1992

A Review of Graphite and Gold Surface Studies for Use as Substrates in Biological Scanning Tunneling Microscopy Studies

Carol R. Clemmer
University of Utah

Thomas P. Beebe Jr.
University of Utah

Scanning Microscopy, Vol. 6, No. 2, 1992 (Pages 319-333)
Scanning Microscopy International, Chicago (AMF O'Hare), IL 60666 USA

0891-7035/92$5.00+.00

A REVIEW OF GRAPHITE AND GOLD SURFACE STUDIES FOR USE AS SUBSTRATES IN BIOLOGICAL SCANNING TUNNELING MICROSCOPY STUDIES

Carol R. Clemmer and Thomas P. Beebe, Jr.*

Department of Chemistry and Center for Biopolymers at Interfaces, University of Utah, Salt Lake City, UT 84112

(Received for publication October 31, 1991, and in revised form April 06, 1992)

Abstract

The current status of biological Scanning Tunneling Microscopy (STM) investigations and the importance of using a well-characterized substrate are discussed. The findings of over two years of experiments and over 1,000 images obtained on gold substrates prepared by a variety of different methods are statistically summarized and compared to a very flat reference substrate, highly oriented pyrolytic graphite (HOPG). In an effort to begin to corroborate STM results with those obtained from other more established techniques, the results of Auger Electron Spectroscopy (AES) and Electron Spectroscopy for Chemical Analysis (ESCA) of biomolecular STM samples are presented.

Key Words: scanning tunneling microscopy, highly oriented pyrolytic graphite, gold, Auger electron spectroscopy, electron spectroscopy for chemical analysis, biomolecules, deoxyribonucleic acid

***Address for correspondence:**
Thomas P. Beebe, Jr.
University of Utah
Department of Chemistry
Salt Lake City, UT 84112

Phone: (801) 581-5383
FAX: (801) 581-8433

Introduction

Since Binnig and Rohrer first reported the ability of the STM [8] to image deoxyribonucleic acid (DNA) molecules [9], researchers have continued to investigate the biological applications of the technique. Researchers have been interested in improving the ability of STM to obtain structural information about biomolecules. In early 1989, the capability of STM to resolve the major and minor grooves of uncoated DNA deposited onto HOPG was reported by Beebe, *et al.* [6], and Lee, *et al.* [24]. Dunlap and Bustamante illustrated the possibility that STM could be used to distinguish between the purine and pyrimidine bases of DNA in studies of uncoated poly(dA) molecules deposited onto HOPG and imaged in air [18]. Baldeschwieler and co-workers have presented results suggesting that STM can resolve DNA deposited onto HOPG and imaged in vacuum with atomic detail [17]. Although these results and others [5,6,9,17,18,23,24] have promoted the idea of STM as a technique useful for biological studies, they are not without problems. These problems involve the HOPG substrate upon which these studies were completed [13]. Although the majority of these initial biological STM experiments used HOPG as the substrate, a few researchers have completed their experiments on gold substrates [14,15,25]. A large body of the work completed on gold are *in situ* studies completed by S.M. Lindsay and co-workers.

Now, seven years after the initial suggestion that STM could be applied to study biological systems, progress hinges critically on the need for better understanding of the technique and interpretation of the results. Several papers have discussed some of these ideas previously [7,10,13,33, and personal communications held at the Workshop on STM/AFM and Molecular Biology held at Royaumont Abbey, France, April 1991]. In this paper, the importance of using a well-characterized, atomically flat substrate is discussed. The results of comparative studies of HOPG (which was the substrate used for initial biological studies in this laboratory) and gold substrates, prepared by a variety of documented and spoken methods are presented.

Further, the importance of verifying biological STM results with results collected from the more established techniques of Scanning Electron Microscopy (SEM), Transmission Electron Microscopy (TEM), AES, and ESCA is discussed. The results of the analysis of STM samples by AES and ESCA illus-

trate that depositions of biological molecules, specifically DNA, can be verified using these techniques. Although it has been suggested that Scanning Tunneling Spectroscopy (STS) could be used in principle to differentiate a biomolecule from a substrate feature [1], this has not been demonstrated conclusively in practice. Several researchers have verified their STM work using TEM and SEM [2-4,7,36,37,41]. ESCA has been used by researchers to verify surface modification of their substrate in conjunction with STM results [22,27,40]. STM has been shown to be a complimentary technique to TEM and SEM for the study of biological systems [4,36,41]. With improvements in experiment and theory, important biological questions can begin to be addressed.

Experimental Methods

The STM used in this study consisted of a coaxial double-tube piezo design built at the University of Utah. The design has been described previously in detail [26,42]. Briefly, it consists of an outer piezoelectric tube responsible for sample x, y, z offset and macroscopic initial sample approach, and an inner piezoelectric tube responsible for the x, y, z scanning of the STM tip. The STM is shown schematically in Figure 1. The tips were made of a platinum/rhodium (10% rhodium) alloy wire (0.51 mm diameter), and were prepared by two methods: ac etching [21] or mechanical cutting. All tips were subjected to quality control experiments. Only tips capable of obtaining atomic resolution in preliminary experiments on a freshly cleaved HOPG surface were used in these studies.

The images that are discussed were obtained at room temperature in air at varying tip scan speeds, which are noted with each image. A tunneling current set point of less than 1 nA was used. A differential input preamplifier, in which a "noise" input is electronically subtracted from a "signal plus noise" input, has recently been incorporated into the experimental setup [J. Katz and the LBL STM group are credited for the design of this preamplifier and its incorporation into the STM]. The "noise" input is connected to a wire which makes a path that is nearly identical to the path made by the "signal plus noise" wire leading to the tip. This "noise" wire terminates near the STM tip without making electrical contact. This preamplifier operates with a gain of 0.10 nA/V on a ten volt full scale with a unity gain bandwidth of approximately 2 kHz and a noise level of approximately 2 pA peak-to-peak. The STM was controlled using feedback, scanning, and offset electronics built at the University of Utah, and images were acquired using an 80386/387 based 20 MHz AT compatible computer system equipped with a 12-bit, 150 kHz analog-to-digital converter. Images consist of 256 x 256 arrays of 12-bit data obtained in the constant current imaging mode. Image figures were photographed from the computer screen.

AES and ESCA analyses were performed in a newly constructed ultrahigh vacuum (UHV) surface science chamber designed and built in this laboratory [manuscript in progress, Leavitt AJ, Han T, Clemmer CR, Murphy TE, Beebe TP, Jr. "An Ultrahigh Vacuum Surface Science Chamber with Integral Scanning Tunneling Microscope]. The standard surface analysis equipment (not including the STM) was obtained from Leybold-Heraeus as bolt-on components, which were attached to the custom designed UHV chamber. The UHV chamber has a base pressure of less than 5.0 x 10^{-11} Torr which is achieved with a combination of ion, titanium sublimation, and turbomolecular pumps. A sample transfer interlock facilitates the transfer of samples in and out of ultrahigh vacuum in approximately ten minutes with only a momentary rise of the base pressure. The sample temperature can be varied from 77 K to 1500 K while being monitored with a chromel/alumel thermocouple attached to the sample. The instrumentation and data collection are controlled using data acquisition and graphics programs written in this laboratory. The UHV chamber is shown schematically in Figure 2.

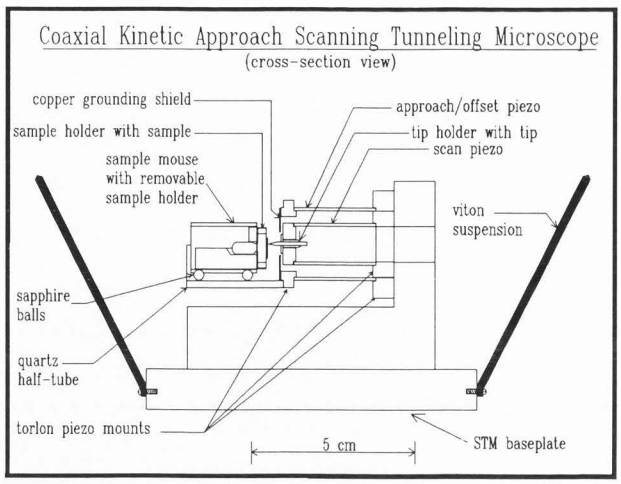

FIGURE 1 - Schematic of the STM assembly in vertical cross-section. Schematic is drawn to scale.

For the analyses presented in this paper, the typical chamber pressure was less than 1 x 10^{-9} Torr, and the plane of the sample was analyzed normal to the entrance axis of the hemispherical kinetic energy analyzer with the electron gun (AES) and the x-ray gun (ESCA) positioned at a 60° angle with respect to the surface normal and working distances of approximately 25 mm. The AES spectra were obtained in the derivative mode at a primary beam energy of 3000 eV and 5 V peak-to-peak modulation of the pass energy. The ESCA spectra were obtained using both $Mg(K_\alpha)$ and $Al(K_\alpha)$ sources at anode powers ranging from 240 W to 390 W (specifics are listed with data).

Individual Sample Preparation

Biological Samples

An 8-mer oligonucleotide with a thiolated guanine (5'-AAAC-S^{6}G-TTT-3') at a concentration of 100 µg/ml (in nanopure H_2O; residual counterions are present - see Verification Studies) was used in these experiments [12]. The DNA was deposited onto a 5 mm diameter flame-annealed Au(111) single crystal (see below) by allowing a 15 µl droplet of the oligonucleotide (covering a circle with an approxi-

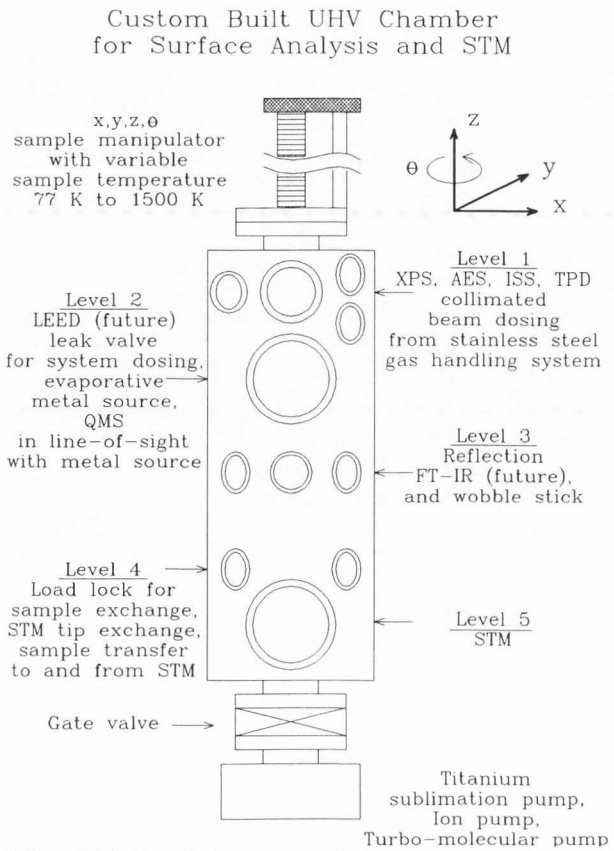

FIGURE 2 - Schematic of the newly constructed UHV surface science chamber designed in this laboratory. The schematic is not to scale, and is meant to show the arrangement of techniques into levels. The total distance from level 1 (surface analytical techniques) down to level 5 (STM) is 50.8 cm.

---

mate diameter of 4.3 mm) to evaporate completely in air. Following the sample preparation, the Au(111) crystal was mounted onto the STM sample holder using two spring-loaded Ta tabs which made contact with the edge of the crystal. The sample was later transferred through the interlock onto the UHV sample holder and analyzed by AES and ESCA.

Gold Films on Mica

The vapor deposited gold films on mica were produced following the procedure of G. Borges [IBM Almaden Research Center, San Jose, CA, from a pamphlet entitled "Epitaxial Metal Films Grown on Mica"]. This procedure has been circulating through the STM community for years with only mixed success. The mica was scratch-free, green mica of ASTM V-2 quality or better (Asheville-Schoomaker Mica Co.). It was cleaved using a scalpel and nanopure water. After cleavage, the mica was placed into an Edwards Coating System evaporator equipped with a thickness monitor, sample heater, and thermocouple. Typical chamber pressure during the deposition was $\leq 2 \times 10^{-6}$ Torr. The mica was

Table 1. Deposition Parameters for Gold Films on Mica

SAMPLE NUMBER	NUMBER IMAGES	SAMPLE TEMP. C°	DEPOSITION RATE Å/SEC	THICKNESS Å	STD. DEV. (AVG.[a])
1	4	25	1	254	15.4
2	18	25	5	933	32.9
3	12	425[b]	5	1001	230.0
4	20	500[b]	5	1000	71.4
5	18	300[b]	1	1005	75.6
6	8	300[b]	1	1005	45.3
7	18	300 ± 23	1	----	54.9
8	18	300 ± 10	1	1315	134.3
9	29	sample #8 after UHV cleaning			131.4
10	2	300 ± 3	1	1009	86.9

[a]For a 7000 Å x 7000 Å image size with the exceptions of samples #2 and #10 which were for a 4000 Å x 4000 Å image size.
[b]No thermocouple in system. Temperature reading obtained by extrapolation of the heating characteristics of a commercial button heater (Spectra Mat).

---

heated (see particulars in Table 1) using a molybdenum button heater (Spectra Mat) and the temperature was monitored with a K-type thermocouple utilizing an ice junction as reference. The thermocouple was spot-welded to one of the two Ta tabs used to anchor the sample onto the button heater. After the deposition, the mica, now coated with a thin gold film, was removed from the chamber and mounted on a sample holder for analysis by STM. Some of the gold film/mica samples were placed into the UHV chamber for AES and ESCA analysis. Since there is discrepancy in the literature involving the deposition parameters (rate of deposition, temperature, and thickness) [11,19,28,32,38,39, and procedure of G. Borges, IBM Almaden Research Center, San Jose, CA, from a pamphlet entitled "Epitaxial Metal Films Grown on Mica"], various deposition parameter values, outlined in the results and discussion section, have been studied.

Annealed Gold Ball and Respective Crystals

The annealed gold surface was produced by melting pure gold wire (Johnson Matthey, 0.25mm) using the procedure of Schneir, *et al.* [35] and Sashikata, *et al.* [34]. In this technique, gold balls approximately 1 to 3 mm in diameter were produced. Using this technique, it was possible to produce atomically flat (111) terraces of gold with some consistency. These terraces exist on flat facets which can be located using an optical stereo-microscope (x160 magnification - Olympus). After location of a facet, an optical stereo-microscope was used to align the STM tip on the facet's center.

The single crystal gold discs were made from an annealed gold ball. A flat terrace was located using an optical stereo-microscope. The gold ball was oriented on a goniometer for use in a slurry string saw (South Bay Technology) so as to cut the ball in a plane parallel to the located facet. Following the cutting of the ball (creating two gold hemispheres), the single crystal hemisphere was polished with successively smaller alumina or diamond grit, ending with 0.05 micron polishing grit, according to standard metal single crystal polishing procedures. The orientation of the crystal was checked using a Laue camera. Following Laue examination, the crystal hemisphere was mounted on the STM sample holder.

Gold deposited onto Quartz

The gold surfaces used in these investigations were produced following the method of K.H. Besocke [personal communication; a slightly different method

has now been published - see reference 20]. A thin film of chromium was deposited onto a circular quartz window (ESCO Prod., 12.7 mm diameter x 1.60 mm thick) using a dc sputtering source in 8.5 x 10^{-3} Torr of argon. Following the deposition of approximately 50 Å of chromium, the quartz window was placed in the Edwards Coating System described above for thermal deposition of the gold film. Typical chamber pressure during the deposition was $\leq$ 2 x 10^{-6} Torr. The films were deposited at room temperature with a deposition rate of 1 - 2 Å/sec and a typical thickness of 1000 - 2000 Å. After deposition, the quartz piece, now coated with a thin film of chromium followed by a thin film of gold, was mounted onto the STM for analysis. The surface was examined before annealing. Following this examination, the quartz window was supported on a steel holder held in a bunsen burner until it became iridescent. A thermocouple placed approximately 2 mm from the edge of the quartz, spot-welded to a stainless steel plate on which the quartz was held, indicated approximately 600°C. Visual observation in a darkened room indicated that the steel holder and quartz were approximately at the same temperature. A newly published procedure uses 723°C instead of 600°C [20]. After a few seconds, the quartz piece was removed and quenched in methanol (caution should be exercised here since the methanol usually ignites and burns with a nearly invisible flame).

Gold Single Crystals (low miller indices)

The surfaces of three 5 mm diameter gold single crystals, (111), (110), and (100), respectively, were examined. The crystals were cut from 1/4" diameter gold rods (Metal Research, England), oriented using Laue, and mechanically polished. Following the mechanical polishing, the crystals were electropolished [31] (These procedures were completed under the direction of Dr. James McIntyre, who was associated with Bell Laboratories at that time.). Although the majority of the STM studies were completed on the as-received single crystals, the Au(111) surface was examined before and after sufficient cleaning in UHV as well as before and after flame-annealing in a bunsen burner with quenching in methanol. In the UHV chamber, the crystal was cleaned by cycles of Ar^+ sputtering (500 eV, 75 min) and annealing (500°C) until no contamination could be detected by AES. The Au(111) surface that was flame-annealed and quenched in methanol was also examined by AES, ESCA and STM.

Results and Discussion

Substrate Studies

Extensive studies on the surfaces of various conducting materials for use as substrates in biological STM studies have been completed. These studies have been completed over a period of two years, and include over 1,000 STM images. The details of the studies of HOPG were described previously [13]. Based upon the results of these HOPG studies [10,13,33], it was concluded that many ambiguous HOPG surface features could be confused with deposited biomolecules, as illustrated in Figure 3. Thus, it is recommended that another substrate be used for these experiments.

There were several characteristics of HOPG that made it a logical choice as the initial substrate for biological STM investigations such as limited reactivity, low surface roughness (less than 5 Å vertical deviation over hundreds of Å lateral distance), and ease of preparation. Subsequent studies in this laboratory and others have concentrated on various gold surfaces. These gold surfaces were created by a variety of different methods and their ease of preparation and relative surface flatness were compared. Table 2 outlines the methods and the number of images that were collected.

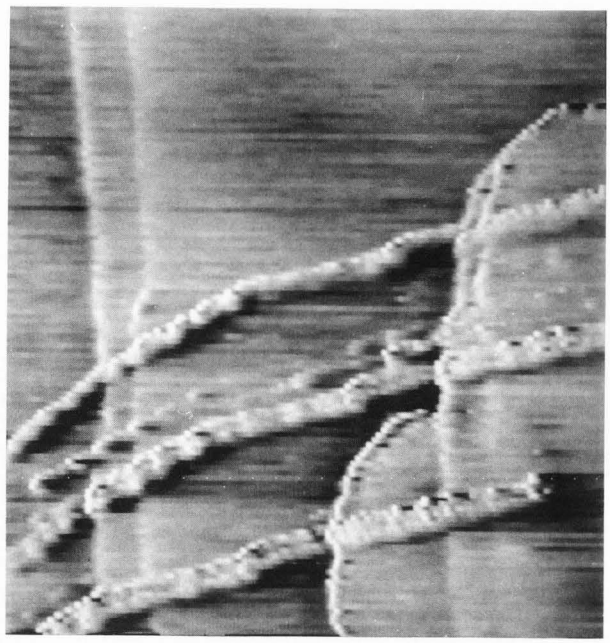

FIGURE 3 - This image illustrates HOPG features that closely resemble biological molecules by their noticeable periodicity and appearance of meandering across HOPG steps. The periodicity is 53 ± 12 Å (obtained from 48 measurements). The image measures 1500 Å x 1500 Å x 37 Å (x, y, z). The scan rate for this image was 6099 Å/sec. No biomolecules were deposited on this surface.

Table 2. Summary of Substrate Preparation Methods

Method	Number of Images Obtained	Literature Reference
I. Gold deposited onto mica	172	[a],11,19,28, 32,38,39
II. Annealed gold ball	70	34,35
III. Single crystal hemispheres cut from annealed gold balls	38	
IV. Low Miller index gold single crystals	532	31
V. Gold deposited onto quartz	52	
VI. Gold/Chromium on quartz	144	b

[a]G. Borges, IBM Almaden Research Center, San Jose, CA, from a pamphlet entitled "Epitaxial Metal Films Grown on Mica"

[b]personal communication with K.H. Besocke; a slightly different method has now been published - see reference 20

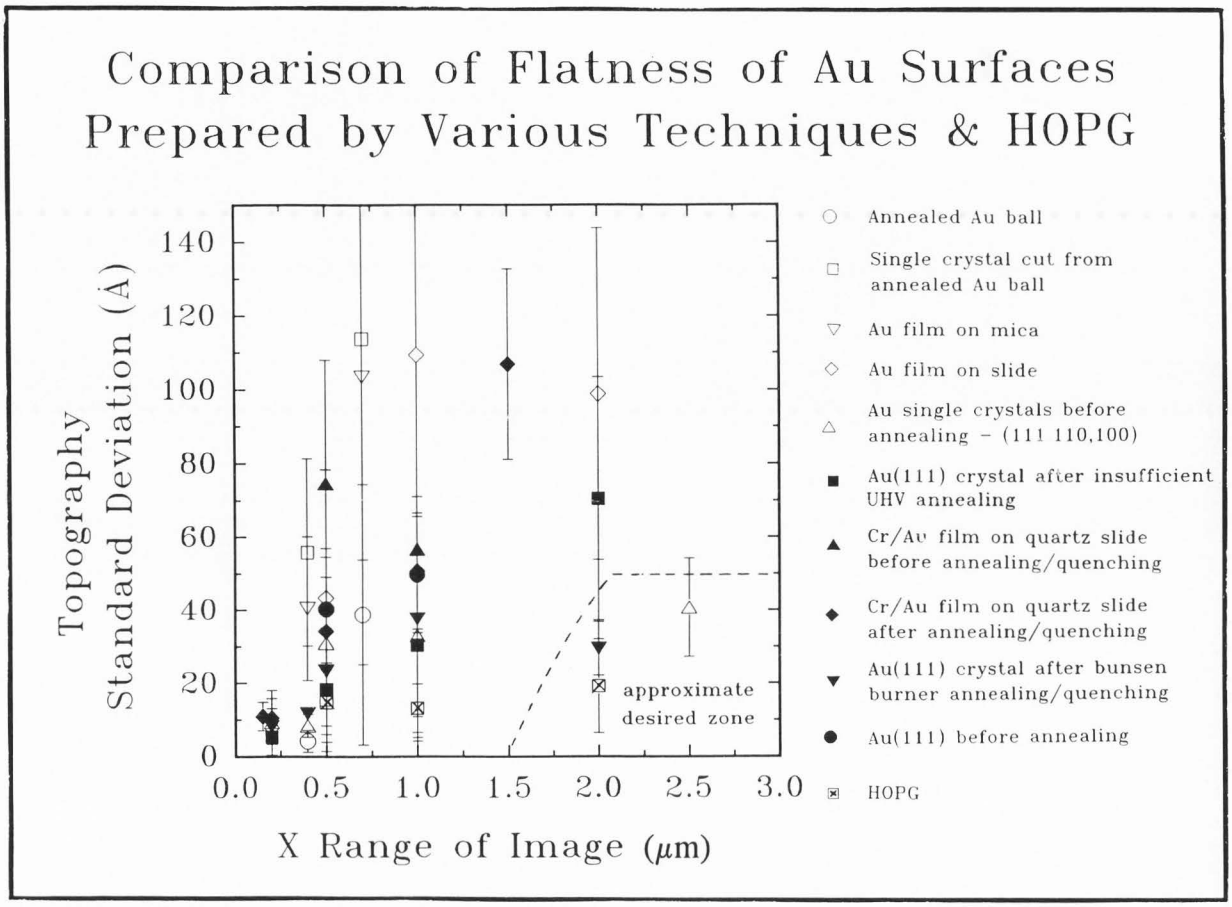

FIGURE 4 - This graph compares the average standard deviation of image topography and respective ranges for each of the gold surface preparation techniques studied and HOPG. The topography standard deviation is obtained by analysis of z-data for all pixels in an image.

Figure 4 compares the average standard deviation of the topography (i.e. z height data) for each technique at various image sizes with those obtained for HOPG. An ideally flat surface extending infinitely in all directions would have standard deviation of zero regardless of image size. Real surfaces, such as those studied, exhibit an increasing relationship between image area and standard deviation in the topography. The greater the image area the more evident the differences between the various surface preparations become. As shown in Figure 4, at image sizes less than 0.5 μm per side, the majority of the surface preparations produce what are apparently relatively flat surfaces. HOPG is the lower limit as far as cost, ease of preparation, and flatness are concerned. As image size grows, the low Miller index single crystals are the closest in comparison to the flatness of the HOPG. These surfaces can be prepared with consistency as evidenced by the small error bars associated with this data. Therefore, a Au(111) single crystal is presently the preferred substrate for biological STM experiments in this laboratory. However, it is important to realize that any surface has the potential for artifacts, and should be thoroughly understood before attempting to interpret images of adsorbed molecules.

Annealed Gold Balls. As others have shown, it is possible to produce atomically flat (111) facets on the annealed gold balls. This technique is relatively inexpensive and easy. However, the experimental geometry of this scheme is limited unless a mechanism exists for convenient x, y positioning on a mm scale. It is especially limited for *in situ* STM experiments. Figure 5 demonstrates a characteristic atomically flat region (Figure 5A) as well as an example of characteristic rougher topography (Figure 5B). The average standard deviation of image topography for an image measuring 4000 Å x 4000 Å is 4 ± 3 Å (obtained from analysis of all pixels in 5 images) and for an image measuring 7000 Å x 7000 Å is 39 ± 36 (obtained from analysis of all pixels in 26 images).

Annealed Gold Ball Single Crystals. Studies of the single crystal discs cut from the annealed gold balls indicate that with significant effort these surfaces could be comparable with the larger commercial low Miller index single crystals of gold. They have the advantage of being relatively inexpensive compared to the large single crystals. However, they are less convenient to work with due to their small size (approximately 1 to 3 mm in diameter) which leads to mounting difficulties in the slurry sting saw and to difficulties in positioning the X-ray spot for Laue analysis. We have found that an unclean and roughly polished surface yields an average standard deviation of topography for an image measuring 4000 Å x 4000 Å of 56 ± 26 Å (obtained from analysis of all the pixels in 4 images) and for an image measuring

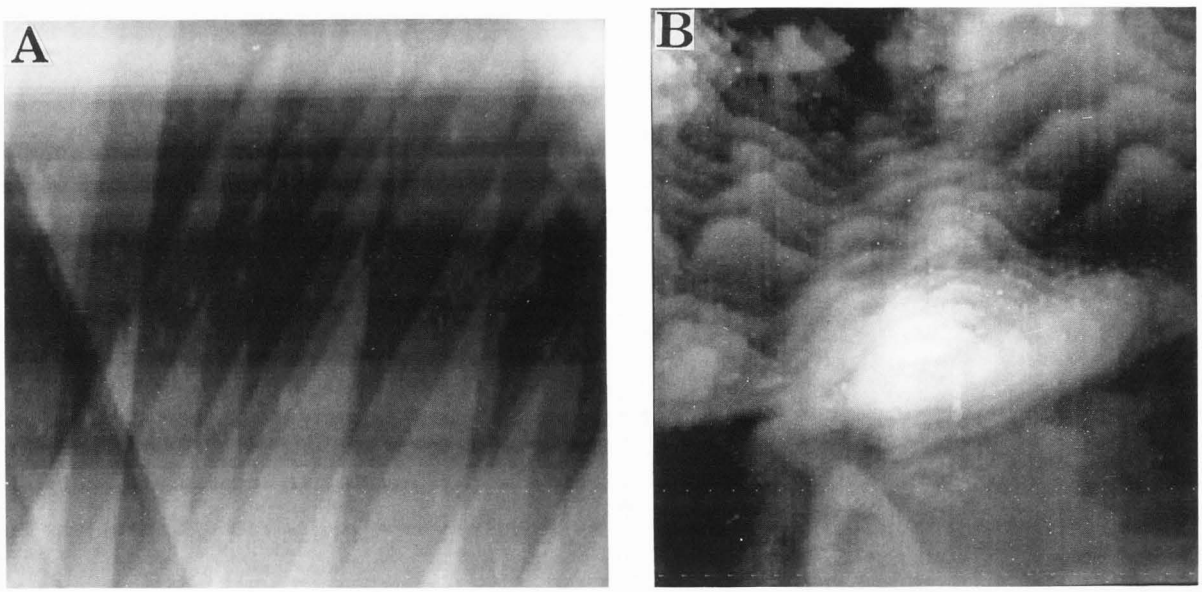

FIGURE 5 - Images of characteristic topography for annealed gold balls **A** - This image illustrates the atomically flat (111) terraces and steps that have been found on the annealed gold ball. This image measures 7000 Å x 7000 Å x 91 Å (x, y, z) and was collected at a scan rate of 2442 Å/sec. **B** - This image illustrates a terraced surface topography ending in flat-topped mesas, which has been found on the annealed gold balls surrounding atomically flat regions. This image measures 3000 Å x 3000 Å x 55 Å (x, y, z). The scan rate for this image was 1832 Å/sec.

7000 Å x 7000 Å a value of 114 ± 60 Å (obtained from analysis of all the pixels in 22 images). Figure 6 illustrates a characteristic image obtained from these surfaces, demonstrating the rough polishing grooves caused by the last polishing grit used. The grooves are locally parallel and are spaced approximately 300-500 Å apart. The occasional spikes appearing as horizontal white streaks result most likely from tip/sample interaction and/or carbon contamination. These samples were not exploited fully, since a more thorough treatment (including sputtering and annealing in UHV) would eventually lead to atomically flat surfaces.

Gold Films on Mica. Several STM studies have been completed on the surface topography of gold films on mica [11,16,19,32,38]. However, a mixture of results has been obtained that suggest that the deposition parameters and film quality are related. Since this technique does produce a surface which can be conveniently incorporated into most experimental STM setups and should produce large atomically flat regions of gold, various deposition parameters that had been reported as effective in the literature were examined [11,19,38,39, and procedure of G. Borges, IBM Almaden Research Center, San Jose, CA, from a pamphlet entitled "Epitaxial Metal Films Grown on Mica"]. Table 1 outlines the parameters studied. In general, these surfaces have been too rough for use as substrates for deposition experiments. STM studies of these substrates have revealed flat islands of varying size surrounded by unpredictable and rough topography. The largest islands exhibiting relatively flat topography (less than 3 Å z height, in some cases) measured approximately 3000 Å in size and were found upon examination of sample #5. This topography is illustrated in Figure 7A. It is true, as discussed by Putnam, *et al.*,

---

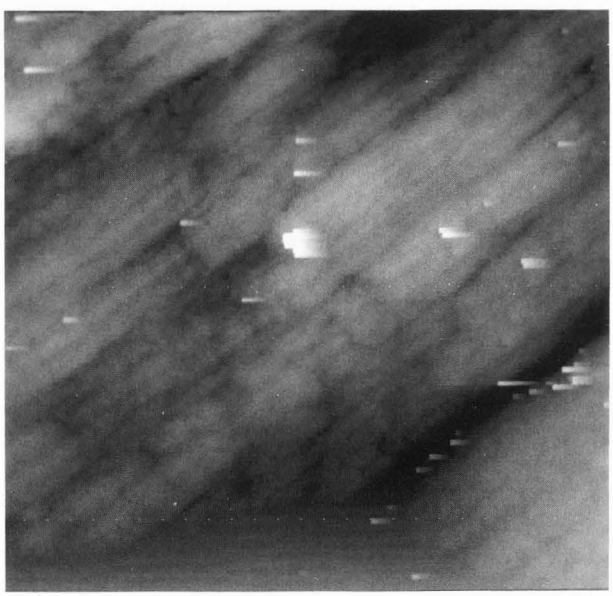

FIGURE 6 - This image illustrates the characteristic topography that has been found when investigating the surface of the annealed gold ball crystal discs. Notice the polishing grooves caused by the last polishing grit used (500 Å grit size). This image measures 7000 Å x 7000 Å x 586 Å (x, y, z) and was collected at a scan rate of 8539 Å/sec.

these islands could be used as a substrate as long as the biomolecule of study was smaller than the island size [32]. However, it was not possible to produce the substrates with grain dimensions of 500 μm reported by G. Borges [IBM Almaden Research Center, San Jose, CA, from a pamphlet entitled "Epitaxial Metal Films Grown on Mica"].

Similar to the results of Putnam, *et al.* [32], Emch, *et al.* [19], and DeRose, *et al.* [16], STM studies of the films indicate a problem with surface contamination. As illustrated by the arrow in Figure 7A, this contamination probably appears as noise spikes in the STM images. These spikes appear predominantly at the edges of the flat islands, and occur at the same place for both scan directions. This surface contamination has been discussed previously as being caused by either poor vacuum conditions during evaporation [32] and/or exposure to air immediately following evaporation [16,19].

AES and ESCA analysis of these films indicate that there was substantial carbon contamination on the as-prepared films after removal from the evaporator chamber (These experiments address contamination which is strongly adsorbed and which would not be removed by simple insertion into UHV. The experiments do not address weakly held contamination which pumps away in UHV.). To investigate whether this contamination was due to the evaporation process or the subsequent exposure to air, these films were analyzed by ESCA and AES. The results of the ESCA analyses following evaporation are presented in Figure 7B, spectrum A, which illustrates the carbon and oxygen contamination. The AES results presented in Figure 7C, spectrum A, illustrate this contamination, also. Emch, *et al.*, discuss the possibility that these films are not stable in air over time [19]. In order to investigate this issue, the initial surface contamination was removed from these films by Ar^+ sputtering and annealing in the UHV chamber. The corresponding clean ESCA and AES spectra are presented in Figures 7B and 7C, spectra B, respectively. These spectra illustrate significantly less carbon and essentially no oxygen contamination. Specifically, notice the change in the carbon-to-gold peak ratio in the AES spectrum. Following this cleaning procedure, the film was removed from the UHV chamber and exposed to the laboratory atmosphere for 2.5 hours. After exposure to atmosphere, the films were reanalyzed by AES and ESCA for contamination. The results of these studies are illustrated in the ESCA and AES results presented in Figures 7B and 7C, spectra C, respectively. There is an increase in the carbon and oxygen peak intensities due to atmospheric exposure, although it is less than what was originally present due to the evaporation. In the AES spectrum (Figure 7C, spectrum C), the carbon to gold peak ratio is significantly lower than the original ratio. Although this study was not carried out over a period of days, it would appear that the films are stable in air over a period of hours with respect to contamination, and that the carbon contamination is deposited during the gold depositions. These results point to the importance of good vacuum conditions during Au deposition which is in contrast with the conclusions made by DeRose and co-workers [16]. They report that chamber pressure during deposition is insignificant for the production of large flat areas, as long as it is below 10^{-5} Torr. Although our pressure during evaporation was 10^{-6} Torr, there was significant problem with contamination occurring during the evaporation. It should be noted that after UHV cleaning of a limited number of samples, the average standard deviation of topography indicates that the surface was rougher than the contaminated surface topography as illustrated in Figure 4. This is true because the surface was probably not annealed long enough after sputtering. With proper sputtering and UHV annealing, a surface could be made atomically flat.

Another problem associated with this technique is the lack of consistency when trying to reproduce film quality from one sample preparation to the next or from one research group to the next. For example, the images presented in Figures 7A and 7D (sample #5 and sample #6 from Table 1) were prepared using identical deposition parameters. However, notice the difference in the topographies. At these deposition parameters according to Borges' procedure [IBM Almaden Research Center, San Jose, CA, from a pamphlet entitled "Epitaxial Metal Films Grown on Mica"] much larger atomically flat islands should have been produced. Discrepancies have also been noted by Vancea, *et al.*, [38] in their inability to reproduce the surfaces reported by Chidsey, *et al.*, [11] even though the deposition parameters were the same. Vancea and co-workers indicate [38] these discrepancies are due most likely to the preparation and quality of the mica before deposition (which is also supported by the findings of DeRose, *et al.* [16]) and possibly to evaporation pressures. Thus, although this technique has the possibility of producing low cost, atomically flat substrates, the issue of reproducibility significantly limits their use as a substrate for biological STM studies. Deposition under UHV conditions is currently being investigated in our laboratory. Results presented by DeRose and co-workers indicate that these conditions should reproducibly produce micron size areas that are extremely flat [16]. They conclude that their success is directly related to the preparation of the mica surface before deposition not chamber pressures during evaporation, deposition rate, or film thickness. In their procedure, the mica is heated for at least 12 hours in UHV prior to deposition to assure a clean surface and annealed during and after deposition at 500°C.

Gold and Chromium/Gold films on Quartz. Initial studies of gold films vapor deposited onto quartz in this laboratory did not involve an underlayer of chromium. These films tended to peel extensively when quenched in methanol following annealing. Thus, the films were no longer continuous across the quartz window. However, STM studies were completed on the individual areas that remained coated. These surfaces had average standard deviations of 43 ± 35 Å (obtained from all the pixels in 16 images), 109 ± 127 Å (obtained from all the pixels in 10 images), and 99 ± 45 Å (obtained from all the pixels in 8 images) corresponding to image sizes of 5000 Å x 5000 Å, 10,000 Å x 10,000 Å, and 20,000 Å x 20,000 Å, respectively.

The gold films that were coated onto a quartz window with an underlayer of chromium were much more stable following annealing. According to the procedure of K.H. Besocke [personal communication; a slightly different method has now been published - see reference 20], this technique should produce large atomically flat regions. To date, the topography of the images obtained suggests that these films

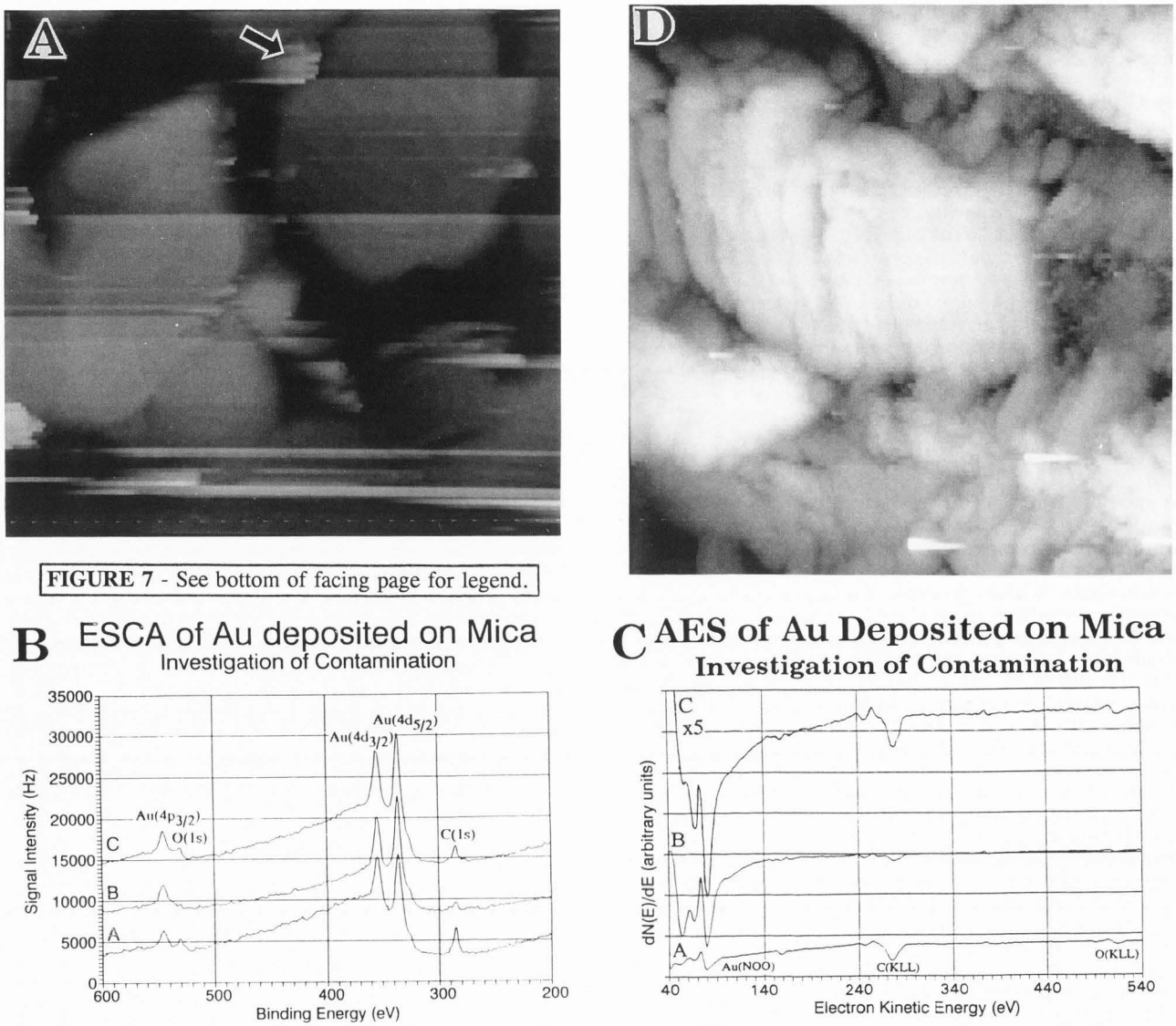

FIGURE 7 - See bottom of facing page for legend.

are unsuitable for use as a substrate. Figure 8 shows characteristic images of the film before (Figure 8A) and after the annealing/quenching process (Figure 8B). As illustrated in Figure 8A, before annealing, the surface topography consists of small gold clusters, typical of the vapor deposition process for Au. The average standard deviation of topography for images measuring 5000 Å x 5000 Å is 75 ± 33 Å (obtained from all of the pixels of 22 images). Larger images were not obtained due to instabilities while imaging. Following annealing and quenching, these films are much flatter and more stable, as illustrated in Figure 8B. Average standard deviations of topography were determined to be 34 ± 20 Å (obtained from all of the pixels of 22 images), 51 ± 16 Å (obtained from all of the pixels of 34 images), and 107 ± 26 Å (obtained from all of the pixels of 12 images) for image sizes of 5000 Å x 5000 Å, 10,000 Å x 10,000 Å, and 15,000 Å x 15,000 Å, respectively. These films are low cost, easy to prepare, and readily adapted to experimental STM setups. Hopefully, with improvements in the preparation of these films, the reported atomically flat surfaces will be able to be produced in the future on a more routine basis. Extensive studies have not yet been completed using the newly published experimental procedure [20].

Low Index Gold Single Crystals. The surface topography of several 5 mm diameter low Miller index gold single crystals, specifically, (111), (110), and (100) were studied. These surfaces are the closest in comparison to the flatness of HOPG, but they have an initial high cost and require tedious preparation and polishing. The majority of the single crystal data presented here was obtained on the as-received crystals, as described in the experimental section (prior to our use, the crystals had been used in electrochemical investigations). Several characteristic images are presented in Figure 9. The average standard deviation of topography for all the crystals before annealing is 31 ± 18 Å (obtained from all the pixels of 10 images), 33 ± 22 Å (obtained from all the pixels of 106 images), and 41 ± 14 Å (obtained from all the pixels of 18 images) for image sizes of 5000 Å x 5000 Å, 10000 Å x 10000 Å, and 25000 Å x 25000 Å, respectively. Notice how the standard deviation in topography is less sensitive to image

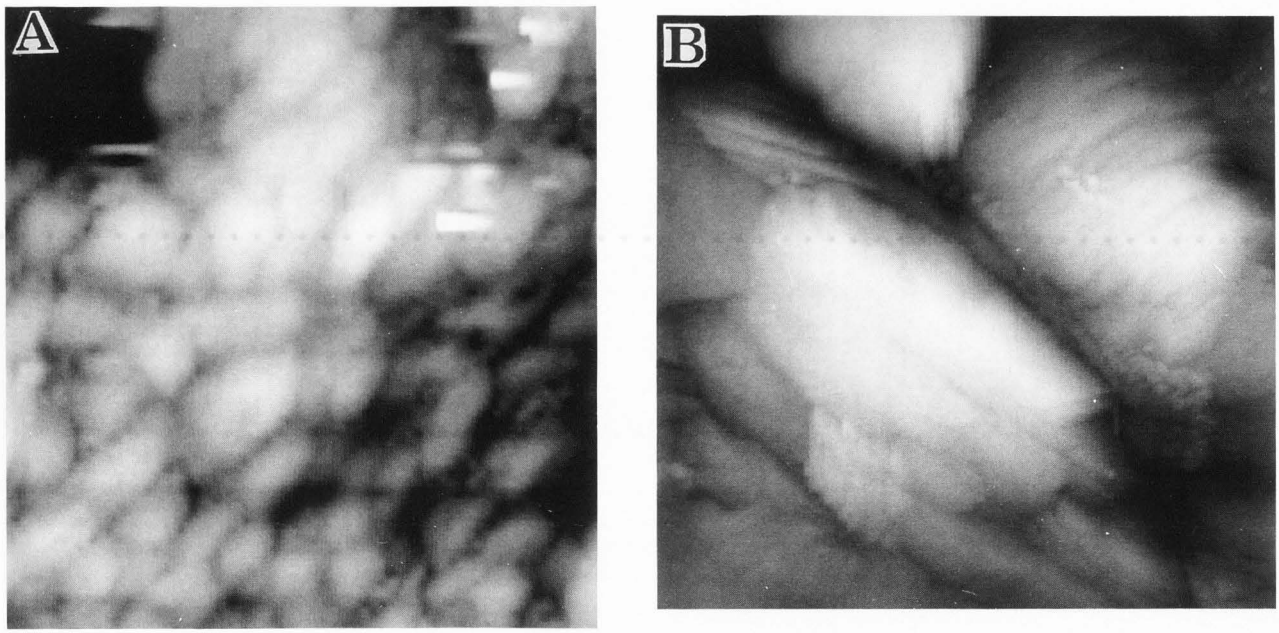

FIGURE 8 - These images are characteristic of the topography found when investigating gold vapor deposited onto chromium coated quartz. **A** - This image is representative of the surface typically found before flame-annealing and quenching in methanol. This image measures 2460 Å x 2440 Å x 402 Å (x, y, z) and was collected at a scan rate of 3050 Å/sec. **B** - This image is characteristic of the surface topography found after flame-annealing and quenching in methanol. This image measures 10000 Å x 10000 Å x 299 Å (x, y, z). This image was collected at a scan rate of 12213 Å/sec.

FIGURE 7 - A - This image illustrates the characteristic gold islands found when investigating the surface of gold vapor deposited onto mica. The size and flatness of the islands depends upon the deposition parameters used. The specific parameters are listed in Table 1 under sample #5. Here, the islands are flat enough for use as a substrate. They measure 3000 Å in diameter and are the largest islands produced. Notice the rough and unpredictable topography surrounding the islands. This image also illustrates the surface contamination that has been adding to the roughness of the topography. This contamination may be the cause of noise spikes in the image (large group marked with an arrow). This image measures 7020 Å x 7020 Å x 715 Å (x, y, z) and was collected at a scan rate of 8566 Å/sec.

FIGURE 7 - B - This plot compares the ESCA data obtained for the gold films vapor deposited onto mica. Spectrum A represents the data obtained for the film following deposition of the gold in the evaporator. Notice the significant contamination of carbon and oxygen present in this spectrum. This spectrum has been displaced by -7000 counts on the vertical axis for clarity in the plot. Spectrum B represents the data obtained after UHV sputtering and annealing. The carbon and oxygen peaks have been significantly decreased relative to the gold. This spectrum has been displaced by +3000 counts on the vertical axis for clarity in the plot. Spectrum C represents the data obtained after the film had been exposed to the laboratory atmosphere for 2.5 hours. Although there is an increase in the intensity of the carbon and oxygen peaks, less carbon and oxygen exist on the surface than the initial amount following the deposition. This spectrum has been displaced by +5000 counts on the vertical axis for clarity in the plot. These spectra were collected using a Mg(k_α) source and anode power of 252 W. **C** - This plot compares the AES data obtained for the gold films vapor deposited onto mica. Spectrum A represents the data obtained for the film following deposition of the gold in the evaporator. Notice the significant contamination of carbon and oxygen present in this spectrum. Spectrum B represents the data obtained after UHV sputtering and annealing. The carbon and oxygen peaks have been significantly decreased compared to the intensity of the gold peak. Spectrum C (shown on a scale expanded by x5 relative to the other spectra) represents the data obtained after the film had been exposed to the laboratory atmosphere for 2.5 hours. The intensities of the carbon and oxygen peaks have increased relative to the gold peak. However, this increase in intensity is less than the initial intensity of these peaks following evaporation. This illustrates that the initial contamination from the evaporation process is more significant than that caused by exposure to the laboratory atmosphere. **D** - The specific deposition parameters for this image are listed in Table 1 under sample #6. Notice that the deposition parameters are the same as were used to produce the film illustrated in Figure 7A. However, the images have quite different topographies. These images illustrate one of the major problems with using gold deposited onto mica as a substrate - the lack of reproducibility. This image measures 7000 Å x 7000 Å x 407 Å (x, y, z). This image was collected at a scan rate of 8545 Å/sec.

---

size, characteristic of an ideally flat surface. AES and ESCA analysis indicate that the as-received Au(111) single crystal had carbon and oxygen contamination. Treatment of this crystal by

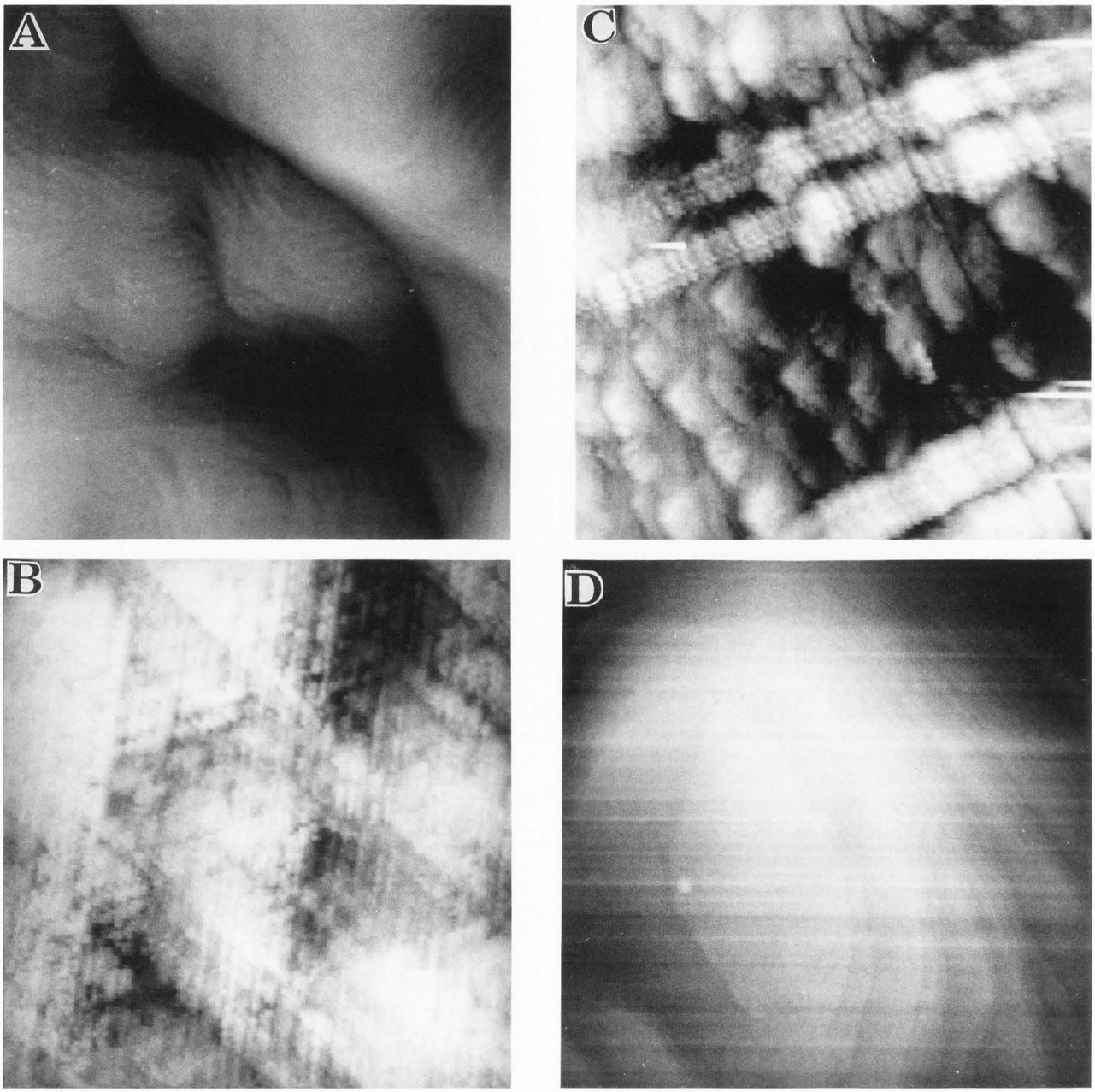

FIGURE 9 - These images are characteristic of the 5 mm low index gold single crystals **A** - This image illustrates the as-received characteristic topography of the Au(100) crystal. This image measures 20100 Å x 20100 Å x 224 Å (x, y, z) and was collected at a scan rate of 15259 Å/sec. **B** - This image illustrates the as-received characteristic topography of the Au(110) crystal. This image measures 10000 Å x 10000 Å x 18 Å (x, y, z) and was collected at a scan rate of 12248 Å/sec. **C** - This image illustrates the characteristic topography of the as-received Au(111) crystal. This image measures 10000 Å x 10000 Å x 255 Å (x, y, z). This image was collected at a scan rate of 12231 Å/sec. **D** - Following annealing and sputtering in UHV, the characteristic topography of the Au(111) crystal improved. This crystal is currently used as the substrate for biological STM studies. This image measures 5020 Å x 5030 Å x 73 Å (x, y, z) and was collected at a scan rate of 12260 Å/sec.

---

sputtering and annealing in UHV or by flame annealing in air and quenching in methanol generally improved the surface flatness - see Figure 9C and 9D for images of the (111) surface before and after annealing. The standard deviation of topography improved by at least 24% for 10000 Å x 10000 Å images, while images of 5000 Å x 5000 Å improved by at least 42%. The UHV annealing procedure produced the flattest surfaces with improvements of 39% and 55%, respectively. These results could be a consequence of the fact that AES and ESCA analysis of UHV annealed crystals

indicate no carbon and oxygen contamination while flame-annealed crystals do possess small amounts of this contamination, which most likely shows up as the spikes in the STM images, increasing the standard deviation.

HOPG Studies. The topography of HOPG surfaces has been a topic of controversy in the field of biological STM because of complicating surface artifacts. Results of studies completed on this surface have been presented previously [10,13,33]. As Figure 4 indicates, this surface represents the most ideal surface studied in terms of flatness and reproducibility of flatness (note the small error ranges). The average standard deviation of topography is 15 ± 11 Å (obtained from all the pixels of 6 images), 13 ± 7 Å (obtained from all the pixels of 20 images), and 19 ± 13 Å (obtained from all the pixels of 22 images) for image sizes of 5000 Å x 5000 Å, 10000 Å x 10000 Å, and 20000 Å x 20000 Å, respectively. It is also the easiest to prepare and involves the lowest cost. However, as the cited works indicate, there are many ambiguous features associated with this surface which make it undesirable for use in these experiments [10,13,15,33].

Verification Studies

It is our opinion that more established techniques should be employed to verify STM and AFM experiments on biomolecules, an opinion that is shared by many researchers in the field [4,7,22,36,37,41]. Studies of modified DNA oligonucleotides have been begun. An 8-mer thiolated DNA has been deposited onto a Au(111) single crystal. It is hoped that the sulfur modification will serve two roles: 1.) aid in adsorption of the biomolecule to the Au substrate, and 2.) serve as a label for the presence of the DNA (when adsorbed on a clean Au surface), to be detected by surface sensitive methods. In initial studies of biological molecules deposited onto HOPG, both air dried and in solution, problems were experienced with tip/biomolecule interactions causing the biomolecules to move on the surface. Biomolecule/substrate interactions could be enhanced because of the soft acid/soft base interactions of the sulfur with the gold [30,39]. In addition, the presence of sulfur as a label on the biomolecule is important since sulfur is not likely to be present from other sources when the Au has been previously cleaned and verified in UHV [29]. Since a better knowledge of STM and the conditions necessary for its application to biological studies is sought, a reproducible technique for depositing these biomolecules onto a substrate is desired which is the subject of ongoing experiments [results to be published in Clemmer CR, Leavitt AJ, Beebe TP, Jr. "Comparative AES and ESCA studies of biological deposition methods for use with STM", manuscript in progress]. AES and ESCA experiments have been conducted to confirm that the oligomers were deposited onto the surface, and to investigate the level of sensitivity required to detect the sulfur label. The results of the ESCA studies are presented in Figure 10. The results indicate that with sufficient signal averaging ESCA can be used to verify the presence of DNA on the surface. There is presently no evidence to suggest that the DNA is spread uniformly on the surface in a manner appropriate for STM and AFM studies, merely that it is present. Experiments are underway to ascertain chemical

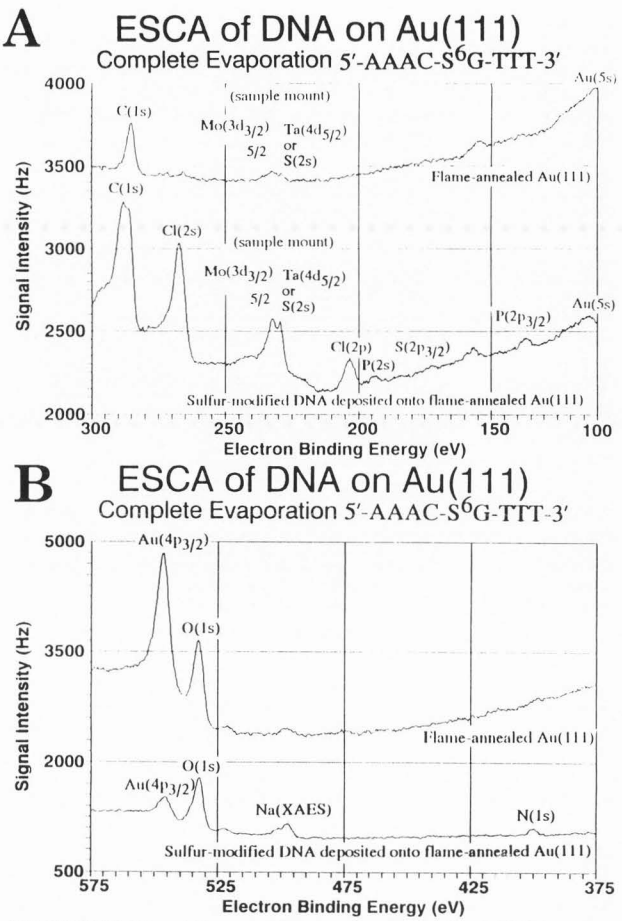

FIGURE 10 - These plots compare the ESCA data obtained for both a flame-annealed Au(111) crystal and sulfur-modified DNA evaporated from solution onto a flame-annealed Au(111) crystal. This data indicates that with sufficient signal averaging ESCA can be used to verify the presence of DNA on the surface. These spectra were signal averaged 50 times. **A** - Comparison of the ESCA data in the binding energy range of 300-100 eV. This range includes peaks representing the phosphorus, carbon and sulfur characteristic of DNA as well as chlorine peaks associated with the counter ion present in the DNA solution. This data was collected using a Mg(k_α) source and anode power of 253 W. The upper spectrum was displaced by +1000 counts on the vertical axis for clarity in the plot. **B** - Comparison of the ESCA data in the binding energy range of 575-375 eV. Notice the nitrogen peak and the x-ray induced sodium Auger peak. This data was collected using an Al(k_α) source and anode power of 381 W. The lower spectrum was displaced by -200 counts on the vertical axis for clarity in the plot.

---

shifts in binding energies to detect the formation of a Au-S chemisorption bond, and to test the integrity of the deposited DNA molecule. As illustrated in Figure 10A, comparison of the spectra for a flame-annealed Au(111) crystal (top spectrum) and for DNA deposited onto a flame-annealed Au(111) crystal (bottom spectrum) in the range of 300-100 eV binding energy indicates that the characteristic

peaks of DNA can be distinguished. These peaks include phosphorus, carbon (notice the increase in intensity over background), and sulfur as well as chlorine peaks which are representative of residual counter ion present in the DNA solution. Peak intensities would need to be corrected for sensitivity in order to make quantitative statements. Experiments addressing this issue are in progress. The molybdenum and tantalum peaks are related to the sample holder used for these experiments, and can be disregarded or used as an internal calibration standard for the energy scale. In future experiments, a brominated oligonucleotide will be used to eliminate spectral overlap of Au with the S label. In the range of 575-375 eV binding energy (Figure 10B), notice the presence of nitrogen and the increase in oxygen intensity when comparing the DNA with the clean Au(111) surface prior to deposition, especially relative to the Au $4p_{3/2}$ peak.

The results of the AES studies are presented in Figure 11. This figure presents the spectra for both a flame-annealed Au(111) crystal (spectrum F) and DNA completely evaporated onto a flame-annealed Au(111) crystal (spectra A-E). Here, the characteristic peaks are gold (69 eV), carbon (272 eV), nitrogen (379 eV) and oxygen (503 eV). There is a relatively small amount of carbon and oxygen present in the AES spectrum of the clean gold as compared to the spectra of DNA on gold. Notice the decrease in intensity of the carbon peak over time in spectra A thru E which is indicative of electron stimulated desorption and/or decomposition (ESD) caused by the 3 keV electron beam. The intensity in the C(KLL) Auger peak increased upon moving the electron beam to a new position. This effect will be discussed in a future paper [results to be published in Clemmer CR, Leavitt AJ, Beebe TP, Jr. "Comparative AES and ESCA studies of biological deposition methods for use with STM", manuscript in progress].

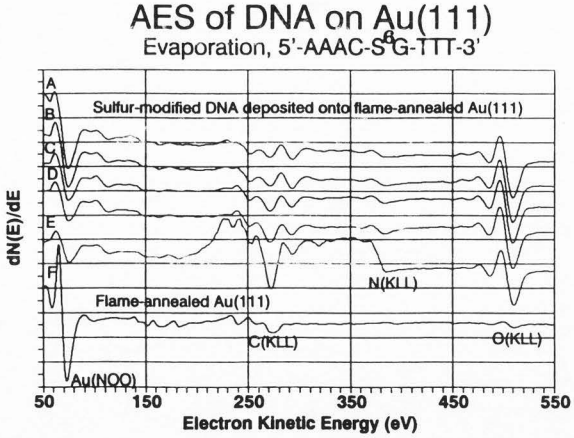

FIGURE 11 - This plot compares the AES data obtained for both a flame-annealed Au(111) crystal (spectrum F) and DNA evaporated from solution onto a flame-annealed Au(111) crystal (spectra A-E). Notice the difference in peak intensities of gold (69 eV), carbon (272 eV), and oxygen (503 eV). Also, notice the ESD of carbon in spectra A-E, collected over a 25 minute period in the same area on the sample.

Conclusions

Using the techniques of STM, AES, and ESCA, a review and statistical summary of various gold surface preparation procedures is presented with regard to surface flatness and cleanliness, cost, and ease of preparation. HOPG is used for comparison as a reference flat surface, although it has been shown to be undesirable due to ambiguous surface artifacts. The substrate chosen based on the results presented here is a 5 mm diameter low Miller index gold single crystal. The need to verify biological STM results with other more established techniques has been discussed, and one approach has been examined. It has been shown that the techniques of AES and ESCA can be used to verify the presence of labeled biomolecules on a gold (111) surface. Experiments are underway to correlate STM images of these surfaces with AES and ESCA results.

Acknowledgements

This work is supported by funding from the Center for Biopolymers at Interfaces, University of Utah, a Utah Center of Excellence. We thank Dr. Arthur Broom, Medicinal Chemistry, University of Utah, for the donation of the thiolated and brominated DNA, and Mike Christopherson for its preparation and purification. We thank Dr. Joel Harris, Department of Chemistry, University of Utah, for the use of his Edwards Coating System. We thank Dr. James McIntyre, Department of Material Science and Engineering, University of Utah, for the use of the 5 mm diameter low Miller index gold single crystals. Figure 5 was collected by S. Funk, an NSF undergraduate summer research student (summer 1990). He is to be acknowledged for collecting additional gold ball surface data.

References

1. Allison DP, Thompson JR, Jacobson KB, Warmack RJ, Ferrell TL. (1990) Scanning tunneling microscopy and spectroscopy of plasmid DNA. *Scanning Microscopy*, **4** (3), 517-522.

2. Amrein M, Durr R, Winkler H, Travaglini G, Wepf R, Gross H. (1989) STM of freeze-dried and Pt-Ir-C-coated bacteriophage T4 polyheads. *J. Ultrastruct. Res.* **102**, 170-177.

3. Amrein M, Stasiak A, Gross H, Stoll E, Travaglini G. (1988). Scanning tunneling microscopy of recA-DNA complexes coated with a conducting film. *Science*, **240**, 514-516.

4. Amrein M, Wang Z, Guckenberger R. (1991) Comparative study of a regular protein layer by scanning tunneling microscopy and transmission electron microscopy. *J. Vac. Sci. Technol. B* **9** (2), 1276-1281.

5. Arscott PG, Lee G, Bloomfield VA, Evans DF. (1989) Scanning tunnelling microscopy of Z-DNA. *Nature*, **339**, 484-486.

6. Beebe TP, Wilson TE, Ogletree DF, Katz JE, Balhorn R, Salmeron MB, Siekhaus WJ. (1989) Direct observation of native DNA structures with the scanning tunneling microscope. *Science*, **243**, 370-372.

7. Blackford BL, Jericho MH. (1991) A metallic replica/anchoring technique for scanning tunneling microscope or atomic force microscope imaging of

large biological structures. *J. Vac. Sci. Technol. B* **9** (2) 1253-1258.

8. Binnig G, Rohrer H, Gerber C, Wiebel E. (1982) Surface studies by scanning tunneling microscopy. *Phys. Rev. Lett.* **49**, 57-60.

9. Binnig G, Rohrer H. in Trends in Physics, J. Janta and J. Pantoflicek, Eds. (European Physical Society, The Hague, 1984), 38-46.

10. Chang H, Bard AJ.(1991) Observation and characterization by scanning tunneling microscopy of structures generated by cleaving highly oriented pyrolytic graphite. *Langmuir*, **7**, 1143-1153.

11. Chidsey CE, Loiacono DN, Sleator T, Nakahara S. (1988) STM study of the surface morphology of gold on mica. *Surf. Sci.* **200**, 45-66.

12. Christopherson M, Broom A. (1991) Synthesis of oligonucleotides containing 2'dioxy-6-thioguanosine at a predetermined site. *Nucleic Acid Research*, **19** (20), 5719-5724.

13. Clemmer CR, Beebe TP, Jr. (1991) Graphite: a mimic for DNA and other biomolecules in scanning tunneling microscope studies. *Science*, **251**, 640-642.

14. Cricenti A, Selci S, Felici AC, Generosi R, Gori E, Djaczenko W, Chiarotti G. (1989) Molecular structure of DNA by scanning tunneling microscopy. *Science*, **245**, 1226-1227.

15. DeRose JA, Lindsay SM, Nagahara LA, Oden PI, Thundat T, Rill RL. (1991) Electrochemical deposition of nucleic acid polymers for scanning probe microscopy. *J. Vac. Sci. Technol. B*, **9** (2), 1166-1170.

16. DeRose JA, Thundat T, Nagahara LA, Lindsay SM. (1991) Gold grown epitaxially on mica: conditions for large area flat faces. *Surface Science*, **256**, 102-108.

17. Driscoll RJ, Youngquist MG, Baldeschwieler JD. (1990) Atomic-scale imaging of DNA using scanning tunnelling microscopy. *Nature*, **346**, 294-296.

18. Dunlap DD, Bustamante C. (1989) Images of single-stranded nucleic acids by scanning tunnelling microscopy. *Nature*, **342**, 204-206.

19. Emch R, Nogami J, Dovek M, Lang CA, Quate CF. (1989) Characterization of gold surfaces for use as substrates in scanning tunneling microscopy studies. *J. Appl. Phys.* **65**, 79-84.

20. Haiss W, Lackey D, Sass JK, Besocke KH. (1991) Atomic resolution scanning tunneling microscopy images of Au(111) surfaces in air and polar organic solvents. *J. Chem. Phys.* **95** (3), 2193-2196.

21. Heben MJ, Dovek M, Lewis NS, Penner R, Quate C. (1989) Preparation of STM tips for *in situ* characterization of electrode surfaces. *J. Microscopy*, **152**, 651-661.

22. Heckl WM, Kallury KMK, Thompson M, Gerber C, Horber HJK, Binnig G. (1989) Characterization of a covalently bound phospholipid on a graphite substrate by X-ray photoelectron spectroscopy and scanning tunneling microscopy. *Langmuir*, **5**, 1433-1435.

23. Keller D, Bustamante C, Keller RW. (1989) Imaging of single uncoated DNA molecules by scanning tunneling microscopy. *Proc. Natl. Acad. Sci. U.S.A.* **86**, 5356-5360.

24. Lee G, Arscott PG, Bloomfield VA, Evans DF. (1989) Scanning tunneling microscopy of nucleic acids. *Science*, **244**, 475-477.

25. Lindsay SM, Thundat T, Nagahara L, Knipping U, Rill RL. (1989) Images of the DNA double helix in water. *Science*, **244**, 1063-1064.

26. Lyding JW, Skala S, Hubacek JS, Brockenbrough R, Gammie G. (1988) Design and operation of a variable temperature scanning tunnelling microscope. *J. Microscopy*, **152**, 371-378.

27. Lyubchenko YL, Lindsay SM, DeRose JA, Thundat T. (1991) A technique for stable adhesion of DNA to a modified graphite surface for imaging by scanning tunneling microscopy. *J. Vac. Sci. Technol. B*, **9** (2), 1288-1290.

28. Mazur U, Fried G, Hipps KW. (1991) Deposited metal films for imaging in scanning tunneling microscopy. *Surface Science*, **243**, 179-192.

29. Musket RG, McLean W, Colmenares CA, Makowiecki DM, Siekhaus WJ. (1982) Preparation of atomically clean surfaces of selected elements: a review. *Appl. Surf. Sci.*, **10**, 143-207.

30. Nuzzo RG, Zegarski BR, Dubois LH. (1987) Fundamental studies of the chemisorption of organosulfur compounds on Au(111). Implications for molecular self-assembly on gold surfaces. *JACS.*, **109**, 733-740.

31. Peck WF, Nakahara S. (1978) Preparation and electropolishing of thin gold disc specimens for transmission-electron-microscope examinations. *Metallurgy*, **11**, 347-354.

32. Putnam A, Blackford BL, Jericho MH, Watanabe MO. (1989) Surface topography study of gold deposited on mica using scanning tunneling microscopy: effect of mica temperature. *Surf. Sci.*, **217**, 276-288.

33. Salmeron M, Beebe TP, Odriozola J, Wilson T, Ogletree DF, Siekhaus W. (1990) Imaging of biomolecules with the scanning tunneling microscope: problems and prospects. *J. Vac. Sci. Technol. A*, **8** (1), 635-641.

34. Sashikata K, Nagakazu F, Itaya K. (1991) *In Situ* electrochemical scanning tunneling microscopy of single-crystal surfaces of Pt(111), Rh(111), and Pd(111) in aqueous sulfuric acid solution. *J. Vac. Sci. & Technol. B*, **9** (2), 457-464.

35. Schneir J, Sonnenfeld R, Marti O, Hansma PK, Demuth JE, Hamers RJ. (1988) Tunneling microscopy, lithography, and surface diffusion on an easily prepared atomically flat gold surface. *J. Appl. Phys.*, **63**, 717-721.

36. Stemmer A, Hefti A, Aebi U, Engel A. (1989) Scanning tunneling and transmission electron microscopy on identical areas of biological specimens. *Ultramicroscopy*, **30**, 263-280.

37. Travaglini G, Rohrer H, Amrein M, Gross H. (1987) Scanning tunneling microscopy on biological matter. *Surface Science*, **181**, 380-390.

38. Vancea J, Reiss G, Schneider F, Bauer K, Hoffmann H. (1989) Substrate effects on the surface topography of evaporated gold films - a scanning tunneling microscopy investigation. *Surf. Sci.*, **218**, 108-126.

39. Widrig CA, Alves CA, Porter MD. (1991) Scanning tunneling microscopy of ethanethiolate and n-Octadecanethiolate monolayers spontaneously adsorbed at gold surfaces. *JACS*, **113** (8), 2805-2810.

40. Wilson TE, Murray MN, Ogletree DF, Bednarski MD, Cantor CR, Salmeron MB. (1991) Scanning tunneling microscopy at high gap resistances and on chemically modified silicon surfaces. *J. Vac. Sci. Technol. B*, **9** (2), 1171-1176.

41. Wepf R, Amrein M, Burkli Urs, Gross H. (1991) Platinum/iridium/carbon: a high-resolution shadowing material for TEM, STM, and SEM of biological macromolecular structures. *J. Microscopy*, **163** (1), 51-64.

42. Zeglinski DM, Ogletree DF, Beebe TP, Hwang RQ, Somorjai GA, Salmeron MB. (1990) An ultrahigh vacuum scanning tunneling microscope for surface science studies. *Rev. Sci. Inst.*, **61**, 3769-3774.

Discussion with Reviewers

S.M. Lindsay: The authors have attempted to quantify contamination on exposure to laboratory air. In contrast to the results presented here, gold contaminates very rapidly (T. Smith, *Colloid and Interface Science*, **75**, 51, 1980) a result consistent with the experience of my laboratory.
Authors: We have quantified the extent of strongly bound contamination resulting from deposition chamber pressures during evaporation and subsequent exposure to air. "Very rapidly" is a term that needs to be defined by an accepted measurement of time, i.e. seconds or minutes. Our paper quantifies both the time scale and the corresponding extent of carbon and oxygen contamination in a manner that could be easily reproduced.

S.M. Lindsay: The authors described the difficulty of assaying the surface for adsorbed DNA using ESCA and Auger methods. It would be much easier to use radiolabeled DNA (^{32}P). It is easier to prepare than thiolated compounds, and trivial to carry out quantitative assays of adsorption.
Authors: We agree that the suggested method would be easier than the experiments that we are completing. In fact, it has been investigated by D.P. Allison and co-workers (Allison DP, Warmack RJ, Bottomley LA, Thundat T, Brown GM, Woychik RP, Schrick JJ, Jacobson KB, Ferrell TL. (1992) Scanning tunneling microscopy of DNA: a novel technique using radiolabeled DNA to evaluate chemically mediated attachment of DNA to surfaces. *Ultramicroscopy*, in press). We are ultimately interested in using ESCA to obtain chemical shift information on the extent of chemisorption bonding of these modified molecules to the surface, which would not be possible using a radioassay.

K.W. Hipps: How many others have observed the stranded structures you report in figure 3? How often have you observed them? The graphite sample appears to have many steps in the relatively small area shown. Has it been oxidized or acid etched in some way? Figure 4 gives an approximate desired zone but does not justify the scale chosen. Further, HOPG samples (probably even the ugly one shown in figure 3) often fall within this zone. More text justifying (or perhaps modifying) the authors choice would be appreciated.
Authors: All the details of images similar to figure 3 as well as our reasons for not using HOPG as a substrate for biological STM and AFM experiments have been described in detail previously. Please see, CR Clemmer and TP Beebe, Jr. (1991) Graphite: a mimic for DNA and other biomolecules in scanning tunneling microscope studies. *Science*, **251**, 640-642.

K.W. Hipps: Figure 9C appears to have stranded structures in it as well. Are these perhaps an experimental artifact?
Authors: As we indicated in the paper, this particular image is illustrative of the as-received Au(111) single crystal (no UHV treatment). As we explicitly state in the paper (underlined in text), any surface has the potential for artifacts.

K.W. Hipps: Many of these pictures required 10 to 25 minutes to obtain. During these long scans, I would expect thermal drift and (especially) creep to distort the images. Could the authors please comment on this?
Authors: Thermal drift can be a factor in longer scans. However, it does not appear to be a significant problem. For example, notice the straight crystallographic lines in figure 5A. If the position of the tip was drifting significantly, we would expect to see curvature in these lines. This scan took 12.2 minutes to obtain. In principle, this STM is constructed so as to self-compensate for thermal drift [42].

K.W. Hipps: Some of the figures (eg., 5A and 9B) have pronounced triangular patterns. Could the authors comment on these?
Authors: The triangular patterns are representative of the crystallographic symmetry of a close-packed (111) surface. Figure 5A illustrates the triangular pattern formed by the crystallographic lines characteristic of a Au(111) surface which is expected of the facets of these annealed gold balls. Figure 9B is an image of a 5mm Au(110) single crystal. We would expect the crystallographic lines to create a pattern containing 90° angles, a manifestation of the rectangular atomic structure. However, the triangular pattern is indicative of (111) which suggests a surface reconstruction from (110) to (111) microfacets. This reconstruction has been examined previously by G. Binnig and co-workers (Binnig G, Rohrer H, Gerber Ch, Weibel E. (1983) *Surface Sci.*, **131**, L379).

K.W. Hipps: There appear to be a large number of tip changes in many of these pictures (figure 7A is particularly bad). If smaller areas are scanned slower, does their frequency go down?
Authors: The tip changes in figure 7A are probably caused by contamination on the surface. If slower scan speeds are used in a region containing no contamination, the tip changes go away. However, changing the scan size and the scan speed has little effect on the tip changes if there is still contamination in the area being scanned.

J.D. Baldeschwieler: Nevertheless, the paper contributes little understanding to the field and presents no novel results.
Authors: Progress in scientific endeavors more often than not procedes by careful work. The goals of our efforts should not focus on novelty. "Unnovel" work is often necessary to provide better overall understanding. As illustrated by another reviewer (R. Balhorn), "Many of the techniques and surfaces used in this study have been reported before. In this paper, however, the authors critically examine multiple samples of a variety of different gold preparations in the context of their usefulness as a substrate for imaging biologically relevant molecules such as DNA...Most of these, including gold, have not

been critically evaluated as substrates. While this task is not as stimulating as the imaging of the molecules themselves, it is an essential step that must be performed."

J.D. Baldeschwieler: One of the problems in a "comparative study" is the need for an objective measure of surface ideality for use as a biological imaging substrate. The authors have used the standard deviation of the surface topography. While this measure is asymptotically appropriate, intermediate values can be ambiguous. Measurements relevant to biomolecular imaging might better be the size of the largest atomically flat regions and the percentages of the surface made up of atomically flat regions whose smallest dimension is greater than 100 Å, 1000 Å, and 1 μm. Unfortunately, this type of analysis would be difficult to perform on a large number of images. While seemingly unscientific, the best measure of substrate quality may still be the subjective answer to the question "how easy would it be to see double-helical DNA if it were on the surface and yielded an STM height response of at least 5 Å?" (Substitute the specimen of choice and use a conservative height response). The "as-received" surfaces of the 5mm Au crystal (Fig. 9a-c) would not be as highly rated for dh DNA imaging as the flame-annealed wire (Fig. 5a) or the annealed single crystal (Fig. 9d).

M. Amrein: I wonder whether the standard deviation is the best measure with which to judge the suitability of a crystalline surface as a specimen support. The standard deviation is very sensitive to the height of crystallographic steps, to their exact location within the image and to long range height variations of the surface, factors that may all be irrelevant to specimen support suitability. Furthermore, discontinuities between adjacent scan lines that certainly represent an imaging artifact (e.g. Fig. 9D) rather than a topographical feature of the sample, affect the standard deviation as well. Possibly, the average size of atomically flat areas as well as their abundance on the surface would be a better measure.

Authors: We agree with both statements. However, as pointed out by J.D. Baldeschwieler, this would be a difficult task for as large a data set as ours. We are of the opinion that the standard deviation, although perhaps not the best measure, is an appropriate and straightforward manner to discuss the surface roughness of these substrates, and hence their suitability as a specimen support.

M. Amrein: The use of different image sizes as well as the different numbers of processed images for each type of sample make it very complicated to compare the relative surface flatness of the differently prepared supports on the basis of their standard deviations (Fig. 4, which should be helpful in this respect, is not easily readable due to overlapping error-bars etc.). I would recommend the use of the same number of processed images for each sample and the use of not more than two different image sizes.

Authors: We agree that Figure 4 attempts to quantify a large amount of data. However, if we were to make the suggested changes, the size of the data set would be significantly decreased and the statistical quality reduced.

R. Balhorn: While both ESCA and AES appear to confirm the presence of DNA in the films prepared on gold in this study, these methods may only prove useful in very limited situations, i.e. studies involving relatively thick molecular films. Have the authors calculated the thickness of the DNA layer in the adsorbate examined in this study? Using the conditions of the preparation described in the paper, my rough calculations indicate that these films must be at least 60+ DNA layers thick. If this is true, it would not appear that either method would be sensitive enough to detect or monitor DNA molecules on a surface at a concentration that would be required to obtain good images of isolated molecules. This point should be addressed in the discussion.

Authors: ESCA and AES can be used to detect a fraction of a monolayer for most elements. The sensitivity of our instrumentation is approximately 0.01 monolayers for well-defined systems on single crystals. We are completing experiments from which we will be able to determine the coverage of the thiolated biomolecules on gold using model thiol systems. A rough calculation indicates that our DNA "film" is approximately 100 monolayers thick based on the size of the molecule (10 Å x 40 Å x 5 Å), concentration, and size of the ring left by the evaporated solution. Since there is one sulfur atom label for each molecule, there is approximately 0.01 of a monolayer of S per monolayer of molecule coverage. In this particular case, there would be approximately 1 monolayer of S distributed throughout the 500 Å thickness of the DNA film. Thus, it might be possible to detect the 0.01 monolayer coverage of S if the concentration of DNA was such that only 1 monolayer of molecules would be deposited, a coverage acceptable for imaging molecules with STM or AFM. However, if a lower concentration of molecules was necessary, label concentration would most likely have to be increased for detection with ESCA or AES. These issues are not as simple as a quick calculation would appear to indicate. Issues of escape depth, molecule packing, and sample degradation must all be considered. Thus, we wanted to postpone our discussion of these issues until after we had completed our coverage studies using model thiolated systems. But, we thank the reviewer for raising the issue.